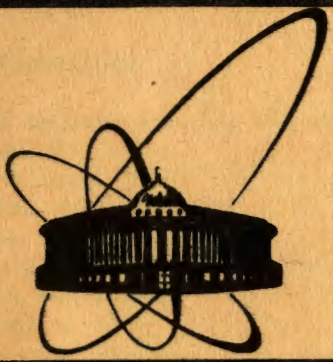

сообщения
объединенного
института
ядерных
исследований
дубна

E2-86-437

V.V.Anisovich[1], M.N.Kobrinsky[2], V.A.Nikonov[1], J.Nyiri

$1/N_c$ EXPANSION, QUARK MODEL AND HADRON COLLISIONS AT HIGH ENERGIES

[1] LNPI, USSR
[2] AURCSV, Moscow, USSR

1986

1. INTRODUCTION

The calculation of soft processes in QCD is so far a rather problematic job connected with all the difficulties of strong interactions. Because of that, it seems to be reasonable to describe these processes with the help of a QCD based phenomenological approach. A possible guide for such a quark-gluon phenomenology of soft processes may be the $1/N_c$ expansion (N_c is the number of quark colours)[3-5].

A description of hadron-hadron collisions which is based on the results of $1/N_c$ expansion is given by the scheme of dual topological unitarization (DTU) - see, e.g.,[6-10] and references therein. The original version of the DTU scheme is suitable if the characteristic size of the gluon interaction is of the order of the hadron size. Supposing the effective short-rangeness of gluon interaction, the DTU scheme leads to a certain hierarchy of contributions: cylindrical graphs which correspond to the impulse approximation of the additive quark model[1,11-13] become the dominating ones, while the other graphs play the role of shadow corrections.

In the present paper high energy hadron collision processes are considered in the case of short range gluon forces. In Part 2 the results of the $1/N_c$ expansion in the quark model which are necessary for our further considerations are briefly reviewed. In Part 3 we investigate the elastic scattering amplitude: we estimate colour shadow effects in πp and pp collisions and discuss the role they possibly play in hadron-nucleus collisions. The inelastic production of fragmentational hadrons is considered in Part 4.

2. $1/N_c$ EXPANSION, SHORT-RANGE GLUON INTERACTION AND THE QUARK MODEL

In the approach of the $1/N_c$ expansion one considers graphs containing large combinatorical factors N_c due to large numbers of intermediate colour states. It is convenient to separate diagrams with different orders of N_c using a substitution of gluon lines by double lines corresponding to quark-antiquark pairs (or, to be more accurate, to colour-anticolour pairs). The difference between the number of coloured gluon states N_c^2-1 and of coloured states of quark-antiquark pairs N_c^2 is negligible within the accuracy given by the approach.

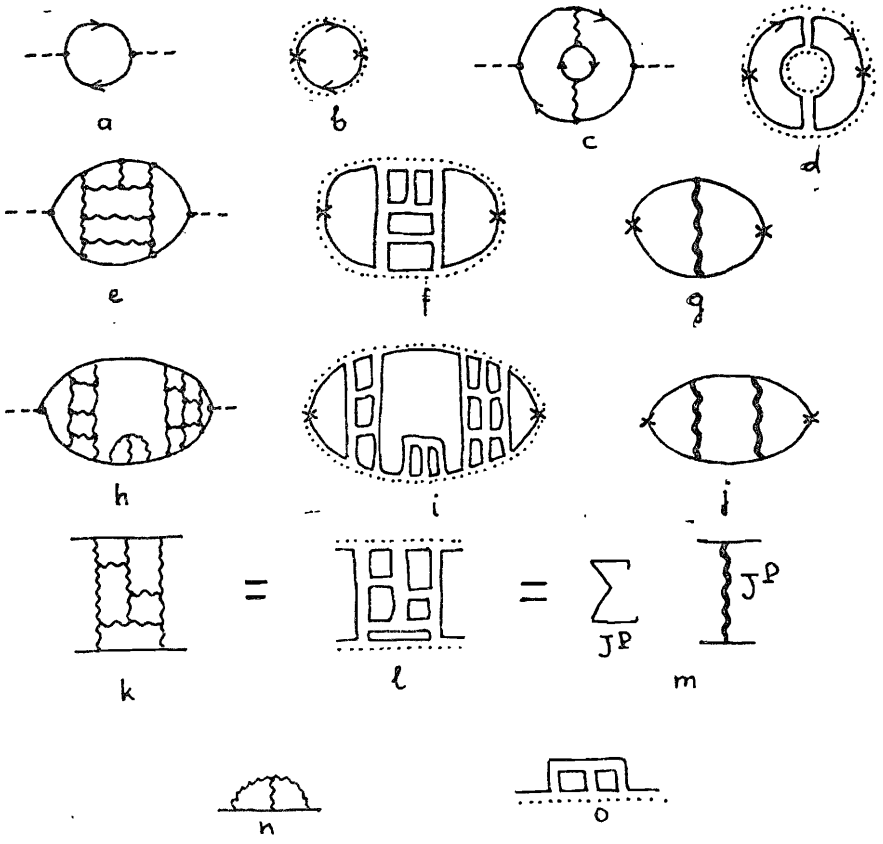

Fig.1. Graphs for self-energy parts of mesons (a-j), quarks (n,o) and blocks of scattered quarks (k-m) described in the language of QCD quarks and gluons (a, c, e, h, k, n), in the language of colour diagrams (b, d, f, i, l, o) and in that of the quark model (g, j, m).

A quark loop, produced by a white source (Fig.1a or, in a different way, Fig.1b) contains a large factor N_c corresponding to N_c colours running around the loop. Bound states can exist only, if the quark-gluon coupling constant is of the order of $g \sim 1/\sqrt{N_c}$. In this case all planar diagrams of the types of Figs.1a, 1e, 1h, etc., are of the same order ($\sim N_c$). This can be seen easily if we redraw these graphs in the form of colour graphs, i.e., substitute gluon lines by double ones (see Figs.1f, 1i - the dotted lines symbolize the path of flavours).

Planar diagrams, containing quark loops (e.g., the graph Fig.1c) are of one order less in N_c (see Fig.1d). However, the internal loop contains quarks of different flavours, consequently, an additional factor N_f arises. Taking into account only light quarks (u, d, s) we have $N_c = 3$ and the graph Fig.1c turns out to be of the same order as all the other planar diagrams. Concerning the role of factor N_f there exist different opinions. For example, from considerations in [5] it follows that N_f is practically irrelevant. On the contrary, in a concrete model which is considered in [14] the factor N_f enhances the contribution of the corresponding diagrams. This shows at least, that there might be cases when N_f is significant. In the present paper we will use this assumption.

Let us discuss now what the quark model means from the point of view of the $1/N_c$ expansion. Suppose, that in the graphs Figs.1a, 1e, 1h the source is a meson field. Consider the corresponding self-energy parts of the meson propagator (they determine the meson masses). One can divide graphs like Figs.1c, 1h into parts which are connected by intermediate states containing only $q\bar{q}$ pairs. In this way one in fact separates blocks inside of which the quarks and the antiquarks interact by gluon exchanges (Fig.1k). For example, the graph Fig.1e contains one such block, graph Fig.1h - two of them.

In the leading approximation in N_c the block with gluon exchanges (Fig.1k) means an exchange of colour states $C = 1 \oplus 8$. Indeed, as it is seen in Fig.1l, the colour exchange between the quarks is carried out by only two colour lines (the main contribution to the number of states is due, naturally, to the colour octet). One can assume, that for the block Fig.1l a sort of dual expansion is valid, and it can be represented by an exchange of effective fields (see Fig.1m). If so, the amplitude V of the block Fig.1k is the sum of propagation functions of these effective fields ($D_{J^P_C}$) with different J^P and C values:

$$V = \sum_{J^P C} B_{J^P C}(s) D_{J^P_C C}(t), \qquad \text{where } D_{J^P C}(t) \sim \frac{1}{m^2(J^P C) - t}. \quad (1)$$

The amplitude V is a function of s - the total energy squared - and of the momentum transfer squared t. Restricting ourselves to the region of low s (the region in which the quark model is assumed to be valid), the coefficients B in (1) can be considered as being nearly independent of s. In this case it is enough to summarize over the lowest values $J^P = 0^-, 0^+, 1^-$, etc., only; the exchange of such effective mesons has to describe the quark interactions in the quark model.

It is known from investigations of potentials that the t-channel exchange of an effective gluon ($J^P = 1^-$, $C = 8$) plays a dominant role in the mass splitting of hadron multiplets [15-17]. Meson spectroscopy shows also that interactions with $J^P = 0^-$ in the white channel are necessary: they lead to the splitting

of η and η' mesons. The role of exchanges with order J^P is not clear so far.

Quark propagators D_q determine the quark masses $D_q \sim \frac{1}{\hat{k} - m_q(k^2)}$. Since the self-energy parts of the quark propagators (Figs.1n, 1c) are not small in N_c, the quark mass $m_q(k^2)$ has to be seriously dependent on k^2. Calculations on the basis of current algebras lead to small mass values of current quarks (i.e., masses at large k^2); $m_u \simeq 4$ MeV, $m_d \simeq 7$ MeV. Estimations show [18,19] that the quark mass increases relevantly at small virtualities $k^2 \sim 0.1$ GeV (which is the region of validity of the quark model) and therefore $m_q(0.1\ \mathrm{GeV}^2) \simeq 300$-$400$ MeV is a fairly plausible value for the mass of a dressed non-strange quark.

In the framework of the quark model graphs lines Figs.1e,1h are represented in the form Figs.1g. 1j. The dressed quark propagators contain the self-energy parts, while the blocks with quark interactions, which correspond to gluon exchanges (of the type Fig.1k) are drawn in the form of effective meson exchanges (fat waved lines).

From the point of view of the $1/N_c$ expansion it is irrelevant, whether the language in which the interaction graphs are written is that of propagator functions of constituent quarks and gluons or of QCD quarks and gluons. The combinatorial factors N_c have to be separated in the same way in both cases; the blocks B in (1) are of the same order as the chromodynamical coupling constant squared g, i.e., $B \sim g^2 \sim 1/N_c$. The meson mases are defined by the poles of the $q\bar{q} \to q\bar{q}$ amplitude, which in the quark model are given by a series of graphs Figs.2a,b,c, etc. The residua of these poles are squared vertex functions (or coupling constants) of the transition "meson $\to q\bar{q}$". It can be seen from Figs.2a,b,c, etc. that the vertex functions G are of the order of $\sqrt{1/N_c}$ and therefore $G \sim \sqrt{B} \sim g$.

In the quark model hadron masses are usually calculated in potential approaches. The considered potentials contain short-range components ($\sim \delta^3(r_{ij})\vec{\lambda}_i\vec{\lambda}_j \frac{\vec{\sigma}_i\vec{\sigma}_j}{m_i m_j}$) as well as long-range ones (which are connected with the confinement of quarks). The hadron masses can be obtained, however, without the consideration of long-range interactions.

The additivity in the quark model is an argument in favour of the relatively small sizes of the constituent quarks and of the effective short-rangeness of gluon interactions (see [20-23]). The latter assumption seems not to contradict QCD [24-26].

Masses of mesons belonging to the lowest multiplets (J^P = = 0^-, 1^-, 0^+) were calculated in [14] assuming short-range gluon forces by solving bootstrap equations for low-energy scattering amplitudes $qq \to qq$ and $q\bar{q} \to q\bar{q}$. The obtained mass values were in

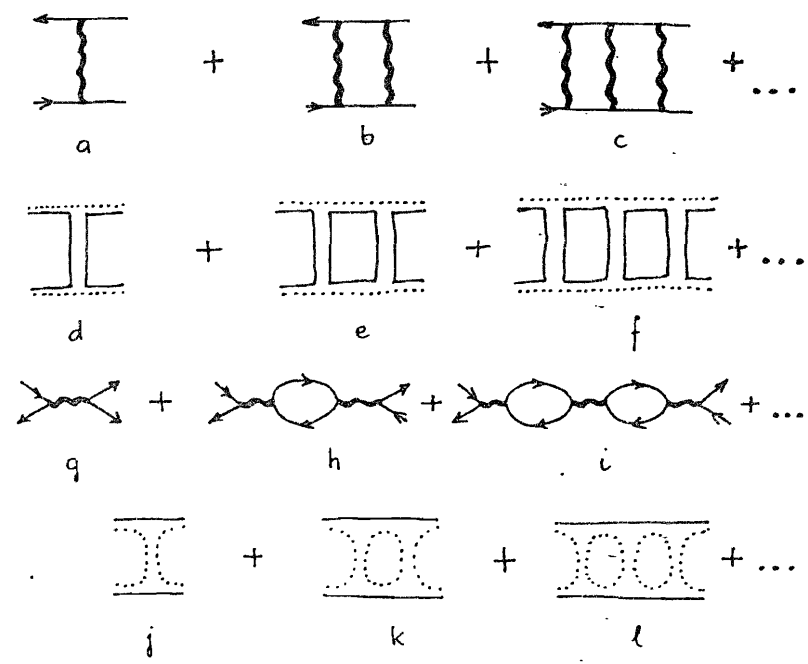

Fig.2. Quarks graphs corresponding to interactions which lead to the formation of mesons (a, b, c,...) and of constituent gluons (g, h, i, ...), and their representation in the form of colour graphs: (d, e, f, ...) and (j, k, l ...) respectively.

satisfactory agreement with experiment. The same calculations indicate the existence of a constituent gluon with a mass $m_g \simeq$ $\simeq$ 700 MeV which is near to the mass of the ρ-meson. This approximate equality $m_g \simeq m_\rho$ is a direct consequence of the relevance of factor N_f. Indeed, the ρ-meson mass can be determined by graphs of the type Figs.2a, b, c, while the gluon mass is defined by diagrams in Figs. 2g, h, i, etc. If gluon forces are short-range ones, these graphs are nearly equal (substituting $N_c \leftrightarrows N_f$). The existence of a constituent gluon with $m_g \simeq 700$ MeV is in agreement with the phenomenology of hard processes [27] and of glueballs [28-30] as well.

3. HADRON-HADRON SCATTERING AT HIGH ENERGIES AND COLOUR SCREENING

As was told already, investigations of hadron collisions using $1/N_c$ expansion were carried out for the general case

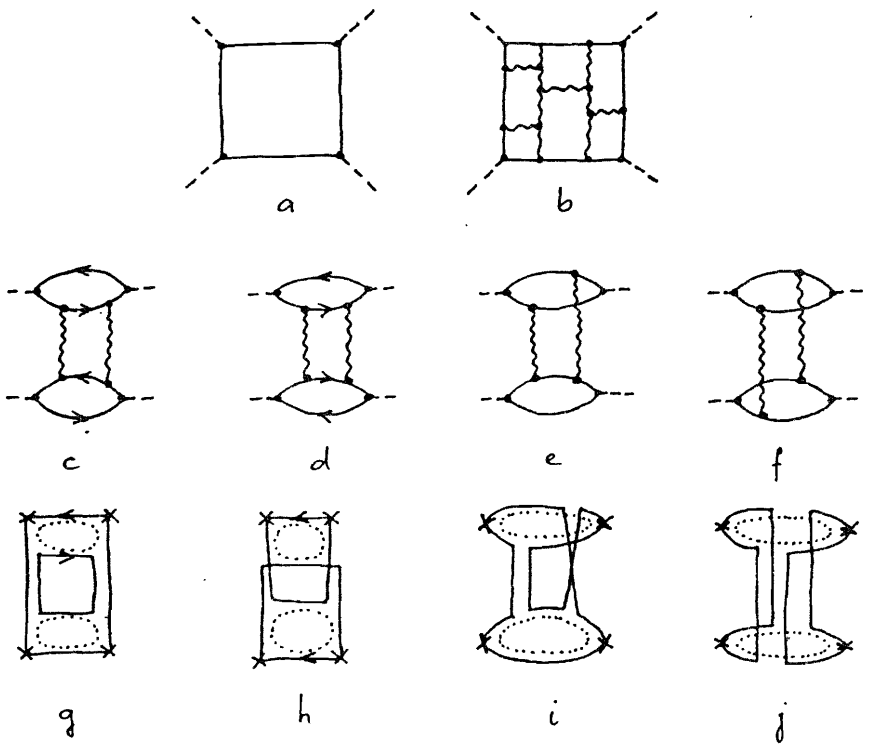

Fig.3. Planar (a, b) and cylindrical graphs ((c-f) - in the quark-gluon language and (g-j) in the form of colour diagrams) for meson-meson scattering.

in the framework of the DTU scheme. The main contribution to the scattering amplitude comes from planar-type graphs (Figs.3a, b), which are of the order $G^4 N_c \sim 1/N_c$ and is interpreted as the contribution of Reggeons like P′, ρ, ω, etc. with the intercept $\alpha_R(0) \simeq 1/2$. At large s values planar type diagrams behave like $\sim\sqrt{s}$. The Pomeron exchange (the contribution of which increases like $\sim s$) corresponds to graph with gluon exchanges in the t-channel. In this case cylinder-type graphs play the main role: a Pomeron is represented by a cylindrical gluon net around the quarks. The contribution in N_c is here $1/N_c^2$. The simplest cylindrical graphs corresponding to two-gluon exchanges are shown in Figs.3c-f.

The assumptions of short-rangeness of gluon interactions (with a radius r_g), leads to different contributions of the cylindrical diagrams depending on r_g^2/R_h^2 (where R_h is the hadron radius). This can be seen in the case of simple graphs like Figs.3c-3f; graphs in Figs.3c,d are of the order of r_g^2,

while graphs Figs.3e,f give $\sim r_g^4/R_h^2$. The situation is equivalent to that which is considered when in composite systems shadow corrections are taken into account. The interactions in Figs.3c, d take place if there is one quark pair, those in Figs.3e, f if there are three or four quarks at a small impact parameter. Such an order of contributions remains valid for the general case also. Graphs in which a cylindrical Pomeron is connected to two quarks only (one of the beam, the other one of the target) play a leading role. These diagrams correspond to the impulse approximation of the additive quark model[1,11-13]. They are of the order of r_g^2. Diagrams with a larger number of quarks (corresponding to shadow corrections) give $\sim r_g^4/R_h^2$.

All this is true, of course, not only for meson-meson scattering, but for meson-nucleon and nucleon-nucleon scattering too. Baryon scattering can be considered similarly with the help of colour graphs, interpreting two quarks belonging to the baryon as a diquark, and understanding now the antiquark colour line as the colour line of the diquark.

The impulse approximation of the quark model describes soft hadron collisions at high energies sufficiently well. It gives for total cross sections of pp and πp collisions $\sigma_{tot}(pp)/\sigma_{tot}(\pi p) = 3/2$ which is fulfilled with a 10% accuracy. However, the calculation of shadow corrections[31-35] in the framework of the model gives $\sigma_{tot}(pp)/\sigma_{tot}(\pi p) < 3/2$ while the experimental value is 1.65.

It follows from our previous considerations, that shadow corrections can be due not only to elastic or quasielastic rescatterings of quarks (which are taken into account in[31-35]), but also to one-cylindrical diagrams when a gluon cylinder is connected with three or more quarks. Such a graph is shown in Fig.4a (or, in the language of Regge-exchanges, in Fig.4b). The main contribution in N_c comes from the three-Reggeon graph $PR(8)R(8)$ (Fig.4d) where R(8) is a colour octet Reggeon ($\sim N_c^{-2}$). Diagrams with exchanges of white states (e.g., the three-Pomeron diagram Fig.4c) lead to contributions of the same order as elastic rescatterings ($\sim N_c^{-4}$). Since the main contribution to the colour forces is given by an effective gluon exchange, it seems to be natural to suppose, that a reggeized gluon R(8)=g exchange will be dominant among the three-Reggeon graphs in Fig.4d. (The reggeization of gluons in QCD is considered in detail in[34-36].

Let us see now, if coloured three-Reggeon exchanges are able to explain the experimentally observed value of $\sigma_{tot}(pp)/\sigma_{tot}(\pi p)$. Consider the ratio of cross-sections in pp and πp collisions in the form

$$\frac{\sigma_{tot}(pp)}{\sigma_{tot}(\pi p)} = \frac{9\sigma_{tot}(qq) - 18\delta(p) - 27\Delta(pp)}{8\sigma_{tot}(qq) - 6\delta(p) - 3\delta(\pi) - 12\Delta(\pi p)} . \qquad (2)$$

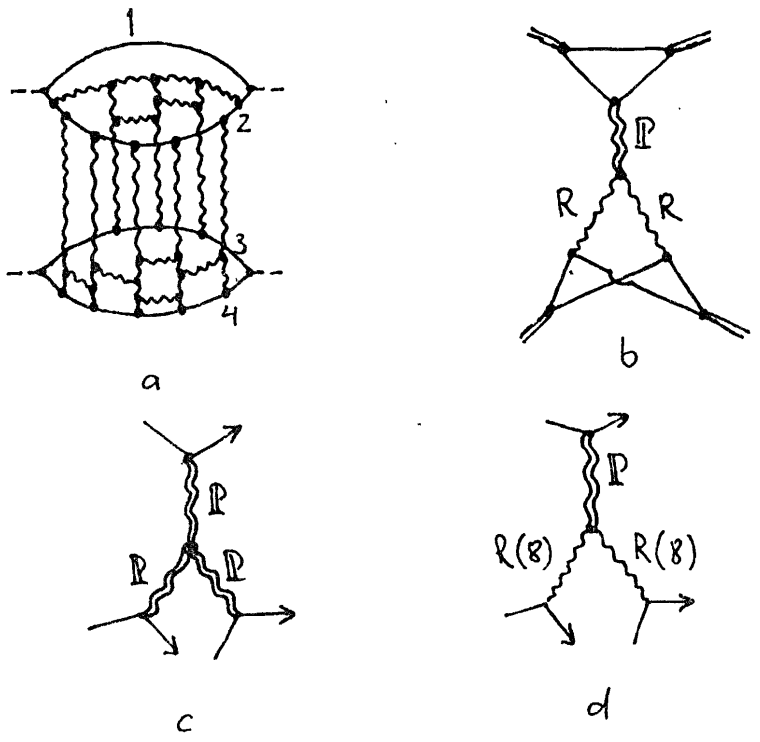

Fig.4. a) Gluon cylinder, connected to the quarks 2,3,4 (quark 1 is a spectator); b) the cylinder graph (a) represented as a three-Reggeon interaction of quarks. The three-Reggeon diagrams, entering graph 4b are: three-Pomeron graph (c) and three-Reggeon graph (d) with the exchange of two coloured Reggeons.

Here $\sigma_{tot}(qq)$ is the interaction cross section of constituent quarks which determines the contribution of the graphs corresponding to the impulse approximation (Figs.5a, 5g), $\delta(p)$ is the contribution of the coloured three-Reggeon exchange in the graphs Figs.5b, 5h and $\delta(\pi)$ - that in Fig.5c, 5i. $\Delta(pp)$ and $\Delta(\pi p)$ are shadow corrections in pp and πp collisions with all possible rescatterings (factors 27 and 12 are due to the number of diagrams with double rescattering - Fig.5d, e, f and Figs. 5j,k,l - which give maximal contributions).

Shadow corrections connected with elastic quark rescatterings were calculated in the spirit of the method given in[37], where in fact inelastic screenings due to white exchanges (of the type of ***PPP*** exchange in Fig.4c) were also taken

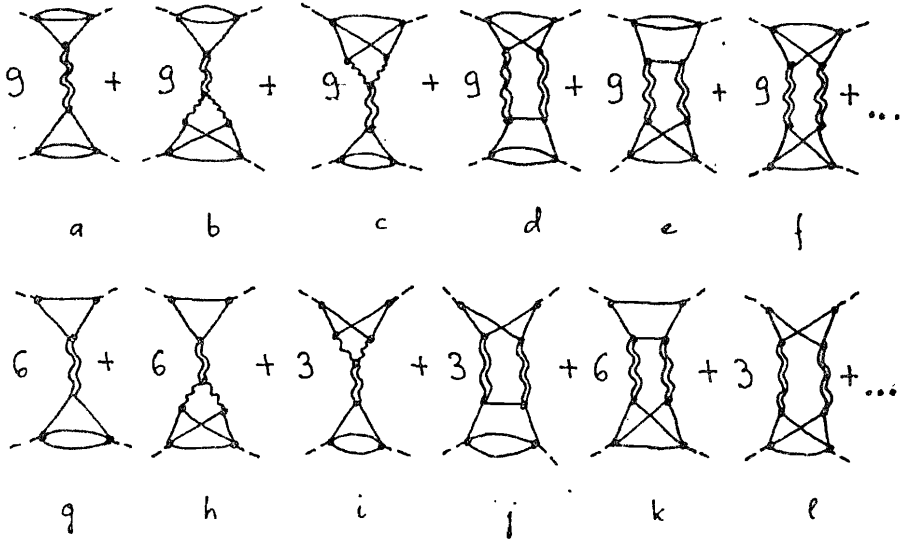

Fig.5. Diagrams determining the cross sections in pp *and* pπ *scattering processes (the numbers stay for the corresponding combinatorial factors). The diagrams a, g are those of the impulse approximation (the double line represents the Pomeron); diagrams b,c,h,i represent three-Reggeon exchanges, diagrams d, e, f, j, k, l - double quark rescatterings. Not in the calculations are triple etc. quark rescatterings.*

into account. The proton and pion quark wave functions were written in the following form:

$$\Psi_p \sim \exp[-\tfrac{2}{3}R_{1p}^2(k_{12}^2+k_{13}^2+k_{23}^2)] + a_p\exp[-\tfrac{2}{3}R_{2p}^2(k_{12}^2+k_{13}^2+k_{23}^2)],$$

$$\Psi_\pi \sim \exp[-\tfrac{4}{3}R_{1\pi}^2 k_{12}^2] + a_\pi \exp[-\tfrac{4}{3}R_{2\pi}^2 k_{12}^2]. \qquad (3)$$

Here $R_{1p}^2 = 21.6$ GeV^{-2}, $R_{2p}^2 = (3.6+0.8)$ GeV^{-2}, $a_p = 0.07+0.02$, $R_{1\pi}^2 = 16.8$ GeV^{-2}, $R_{2\pi}^2 = (1.75+0.8)$ GeV^{-2}, $a_\pi = 0.21+0.07$, and $\vec{k}_{i\ell}$ is the relative quark momentum $\vec{k}_{i\ell} = 1/2(\vec{k}_i - \vec{k}_\ell)$. Such wave functions provide a good description for the proton and pion form-factors up to $Q^2 \leq 0.7$ GeV^2 (the deviation is here not more than $\pm$5%), while in the region at 1 GeV$^2 \leq Q^2 \leq 2$ GeV^2 the deviation is $\pm$(10-30%).

The shadow corrections $\delta(p)$ and $\delta(\pi)$ are determined by three-Reggeon exchanges gg***P***, where g is a reggeized gluon. (Shadow effects connected with three-Reggeon exchanges were investiga-

ted in general in[38-40]). Considering the contribution of ggP it is convenient to separate the factors which one obtains averaging $\vec{\lambda}_i \vec{\lambda}_i$ over the colour states $q\bar{q}$ (in a meson) and qq (in a baryon):

$$\delta_{ggP}(p) = -\frac{2}{3}\delta^{(0)}(p), \quad \delta_{ggP}(\pi) = -\frac{4}{3}\delta^{(0)}(\pi). \tag{4}$$

The signs of $\delta^{(0)}(p)$ and $\delta^{(0)}(\pi)$ depend on the value of the intercept $\alpha_g(0)$ and on the gluon signature. In the case of a negative signature with an intercept $1/2 < \alpha_g(0) < 1$ the values $\delta^{(0)}(p)$ and $\delta^{(0)}(\pi)$ are negative[38-40]; we consider this version, since there are different indications for $\alpha_g(0)$ being small. (In[34,35] there are arguments in favour of $1/2 < \alpha_g(0) < 1$; the formation mechanism of the constituent gluon[14] which was discussed in the previous part of the present paper leads also to $\alpha_g(0) > \alpha_\rho(0) = 1/2$).

The results of our calculations are the following. The value $\sigma_{tot}(pp)/\sigma_{tot}(\pi p) = 1.65$ can be obtained if

$$\sigma_{tot}(qq) \simeq (8{,}5 - 10{,}1)\ \text{mb}, \qquad -\delta^{(0)}(p) \simeq (1{,}0 - 1{,}5)\ \text{mb}. \tag{5}$$

Determined by $\sigma_{tot}(qq)$, $\delta^{(0)}(p)$ and the wave function parameters, the remaining characteristics which enter (2) turn out to be

$$\Delta(\pi p) \simeq (1{,}3 - 1{,}5)\ \text{mb}, \quad -\delta^{(0)}(\pi)/\Delta(\pi p) \simeq 1{,}4 - 1{,}8, \qquad \Delta(pp) \simeq (0{,}9 - 1{,}2)\ \text{mb}. \tag{6}$$

Without the contribution given by colour screening (i.e., $\delta^{(0)}(p) = \delta^{(0)}(\pi) = 0$) the ratio $\sigma_{tot}(pp)/\sigma_{tot}(\pi p)$ does not exceed 1.47.

Let us estimate now, with what probabilities one (q), or two or more (>q) quarks of the projectile hadron interact with the target nucleon. If the projectile is a proton we obtain $W_p(q) : W_p(>q) \simeq 4:1$; if it is a pion, $W_\pi(q) : W_\pi(>q) \simeq 3:1$. These relations show that the consideration of diagrams with only single interactions gives a relatively rough approximation (this we pointed out before, describing the additive quark model - see[37,41]). The colour interaction ggP is responsible for about half of the events when two quarks belonging to a proton are interacting: $W_p^{(colour)}(>q) : W_p(>q) \simeq 0{,}5:1$.

The contribution of ggP is even higher for interactions of two quarks belonging to a pion: $W_\pi^{(colour)}(>q) : W_\pi(q) \simeq 0{,}7:1$.

The shadow corrections in pp and πp collisions break the predictions of the additive quark model by about 10-20%. The situation is probably the same for other hadron-hadron collisions too: the difference between the measured and predicted values of their cross sections are due to shadow corrections, which depend significantly on the radia squared of the colliding hadrons. (Another explanation of the discrepance between experiment and predictions of the additive quark model is given in[42] and references therein).

Taking into account three-Reggeon graphs ggP means practically the account of gluons in hadrons: in fact, gluon components in hadrons are responsible for the breaking of the Levin-Frankfurt relation.

An interesting problem is, how the colour screening manifests itself in high energy hadron and nucleus interactions. Obviously, the colour screening leads to large effects, since quark colours in hadrons are strongly correlated. If quarks are weakly correlated, the contribution of the ggP exchange decreases, while a gas of incorrelated quarks would give a zero ggP contribution ($\vec{\lambda}_i \vec{\lambda}_j \to \mathrm{Sp}\vec{\lambda}_i \cdot \mathrm{Sp}\vec{\lambda}_j = 0$). The absence of colour screening has to lead to an effective growth of the cross section. The analysis of hadron-nucleus collisions at high energies shows, that the cross-sections of hadron-nucleus interactions are somewhat (5-10%) larger than the expected values. This experimental fact might indicate that quarks with weak colour correlations are present in nuclei.

4. MULTIPARTICLE PRODUCTION PROCESSES

As we have already seen, the leading contribution to the elastic meson-meson scattering amplitude at high energies comes from the diagrams of the degenerated cylinder type like those in Figs. 2c,d (or colour diagrams in Fig.2g,h). A more complicated ladder diagram of this type with multiparticle intermediate state is shown in Fig.6a; the equivalent colour diagram is that in Fig.6b.

The cut of the diagram in Fig.6b gives the leading contribution to the inelastic process with production of quarks and gluons (see Fig.6c). The process of hadronization of the produced coloured objects assumes the production of some additional quark-antiquark pairs. Let us consider in more detail the process of hadronization of the constituent quark-spectator (quark 2 in Fig.6c), when it picks up one of the newly produced quarks f and recombines into a meson (Fig.6d). The amplitude of such a recombination process may be easily calculated with

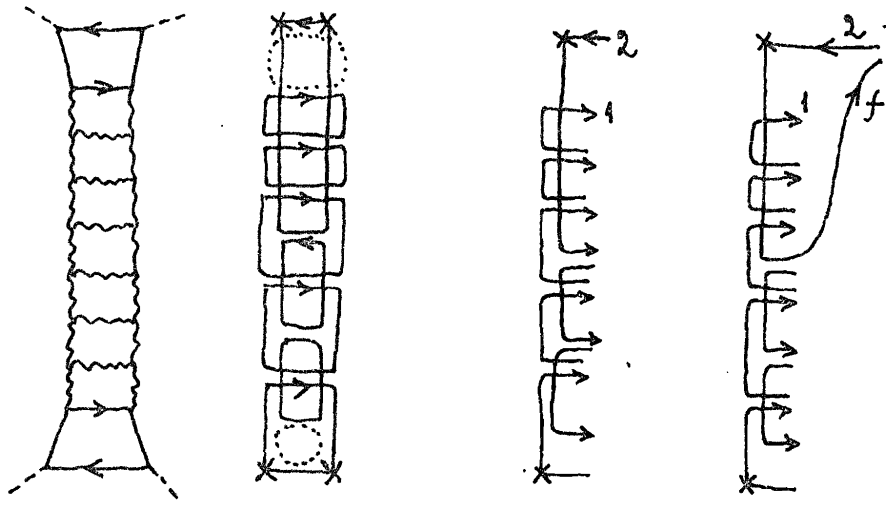

a) b) c) d)

Fig.6. (a) Degenerated cylinder diagram for meson-meson elastic scattering and (b) its representation in the form of colour diagram. (c) Cut of this diagram represents an inelastic process; (d) quark-spectator (2) recombines with a sea quark (f).

the help of dispersion relation technique (see, e.g.,/43/):

$$A_{recomb} = \frac{1}{2}\int \frac{ds\,ds_f}{2\pi\cdot 2\pi}\,\frac{G(s)G(s_f)}{(s-\mu^2)(s_f-\mu_f^2)}\,(2\pi)^4\delta^{(4)}(\vec{P}-k_1-k_2)\times$$

$$\times\frac{d^3k_1}{(2\pi)^3\,2k_{10}}\,\frac{d^3k_2}{(2\pi)^3\,2k_{20}}\,\frac{d^3k_f}{(2\pi)^3\,2k_{f0}}\,(2\pi)^4\delta^{(4)}(\vec{k}-k_f-k_1)\cdot A_{2\to n}\,. \qquad (7)$$

Momentum notations are clear from Fig.6d; $s=\vec{P}^2=(k_1+k_2)^2$, $s_f=\vec{k}^2=(k_2+k_f)^2$, where $\vec{P}=(\sqrt{s+\vec{P}^2},\vec{P})$ and $\vec{k}=(\sqrt{s_f+\vec{k}^2},\vec{k})$. G and G_f are the vertex functions of the transitions "meson → → quarks", μ and μ_f are the initial and final meson masses, correspondingly. $A_{2\to n}$ in eq. (7) is some "quark-quark" inelastic amplitude.

In the infinite momentum frame $P_z\to\infty$, $\vec{P}_\perp=0$ from (7) we get:

$$A_{recomb}=\frac{1}{2}\int\frac{ds\,ds_f}{(2\pi)^2}\,\frac{G(s)G(s_f)}{(s-\mu^2)(s_f-\mu_f^2)}(2\pi)^2\,\frac{dx_1}{x_1}\,d^{2\vec{}}k_{1\perp}\,\frac{dx_2}{x_2}\,d^{2\vec{}}k_{2\perp}\,\frac{dx_f}{x_f}\,d^{2\vec{}}k_{f\perp}\,.$$

$$\times\,\delta^{(2)}(\vec{k}_{1\perp}+\vec{k}_{2\perp})\,\delta^{(2)}(\vec{k}_\perp-\vec{k}_{1\perp}-\vec{k}_{2\perp})\,\delta(1-x_1-x_2)\,\delta(x-x_2-x_f)\times$$

$$\times\,\delta\left(\frac{m_{1\perp}^2}{x_1}+\frac{m_{2\perp}^2}{x_2}-s\right)\delta\left(\frac{m_{2\perp}^2}{x_2}+\frac{m_{f\perp}^2}{x_f}-\frac{s_f+\vec{k}_{f\perp}^2}{x}\right)\cdot A_{2\to n}\,. \qquad (8)$$

Here $x_a=\frac{k_{az}}{P_z}$, $m_{a\perp}^2=\vec{k}_{a\perp}^2+m_a^2$. Killing δ-functions in eq.(8) gives:

$$A_{recomb}(x,k_\perp^2)=\frac{1}{2}\int_0^x\frac{dx_f}{x_f(x-x_f)(1-x+x_f)}\,\frac{d^{2\vec{}}k_{f\perp}}{2(2\pi)^3}\cdot$$

$$G\left(\frac{m_{1\perp}^2}{1-x+x_f}+\frac{m_{2\perp}^2}{x-x_f}\right)G_f\left(x\left(\frac{m_{f\perp}^2}{x_f}+\frac{m_{2\perp}^2}{x-x_f}\right)-k_\perp^2\right) \qquad (9)$$

$$\cdot\,A_{2\to n}\,,$$

$$\left(\frac{m_{1\perp}^2}{1-x+x_f}+\frac{m_{2\perp}^2}{x-x_f}-\mu^2\right)\left(x\left(\frac{m_{f\perp}^2}{x_f}+\frac{m_{2\perp}^2}{x-x_f}\right)-k_\perp^2-\mu_f^2\right)$$

where $\vec{k}_{1\perp}=\vec{k}_{f\perp}-\vec{k}_\perp=-\vec{k}_{2\perp}$.

The inclusive cross section of the meson production with momentum k is given by the square of the amplitude (9) summed over all possible intermediate states. It may be related with the discontinuity of the 3 → 3 amplitude in Fig.7a /43/:

$$\frac{d\sigma_{inel}}{d^3\vec{k}}=\frac{1}{(2\pi)^3\,2k_0}\,\frac{1}{s}\,\mathrm{disc}\cdot A_{3\to A_{3\to 3}}\,, \qquad (10)$$

$$A_{3\to 3}=\int_0^x dx_f\int\frac{d^{2\vec{}}k_{f\perp}}{4(2\pi)^3}\,\frac{1}{x_f(x-x_f)(1-x+x_f)}\,\frac{G(s)G(s_f)}{(s-\mu^2)(s_f-\mu_f^2)}\times$$

$$\times\int_0^x dx_f'\int\frac{d^{2\vec{}}k_{f\perp}'}{4(2\pi)^3}\,\frac{1}{x_f'(x-x_f')(1-x+x_f')}\,\frac{G(s')G(s_f')}{(s'-\mu^2)(s_f'-\mu_f^2)}\times \qquad (11)$$

$$\times\,A_{3\to 3}^{(quark)}(x_1,k_{1\perp};x_1',k_{1\perp}';x_f,k_{f\perp};x_f',k_{f\perp}')\,.$$

In the diagram in Fig.7a P is a white Pomeron, while R is a coloured $1\oplus 8$ exchange state. The amplitude $A_{3\to 3}^{(quark)}$ is given then by the diagram in Fig.7b. We shall consider this amplitude in two kinematic limits: $x\to 1$ and $x=1/2$. Let us begin with the first one.

In the limit $1-x\ll 1$ the invariant energies of quark pairs 1f and 1'f in Fig.7b are small with respect to the total initial invariant energy (of the order of $x_f\sim 1-x$); this means that these quarks interact, producing some effective meson states. On the other hand, the invariant energy in the system

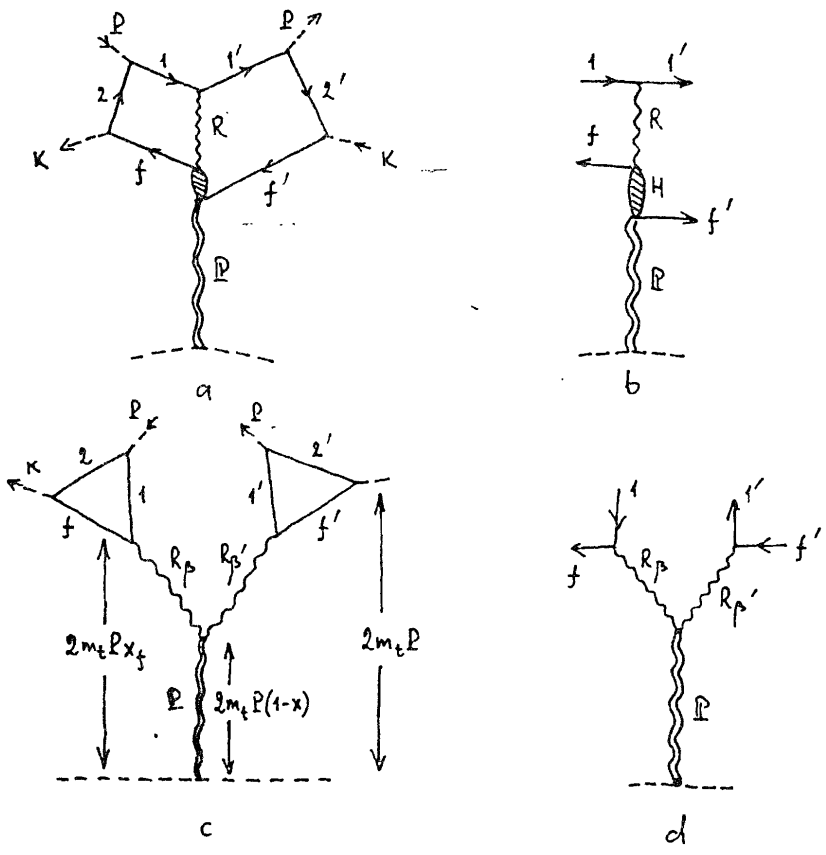

Fig.7. (a) Double-Reggeon diagram for $A_{3\to 3}$ *in eq.(11); (b) the same for* $A^{(quark)}_{3\to 3}$; *(c) three-Reggeon diagram for* $A_{3\to 3}$ *in the* $x\to 1$ *limit; (d) the same for* $A^{(quark)}_{3\to 3}$.

"final meson-Pomeron" is large, since the energy of the Pomeron part of the ladder is also of the order of $1-x$. Thus these effective meson states may be considered as Reggeons, and the diagram in Fig.7a may be presented as a three-Reggeon diagram Fig.7c, or, equivalently, a quark diagram Fig.7b may be redrawn as a three-Reggeon diagram 7d. The corresponding expression for $A^{(quark)}_{3\to 3}$ is:

$$A^{(quark)}_{3\to 3} = \sum_{\beta\beta'} R^{P}_{\beta\beta'}(\vec{k}_\perp^{\,2})(2Pm_t)^{\alpha_P(0)}(1-x)^{\alpha_P(0)-\beta(\vec{k}_\perp^{\,2})-\beta'(\vec{k}_\perp^{\,2})} \times \times (x_f)^{\beta(\vec{k}_\perp^{\,2})}(x'_f)^{\beta'(\vec{k}_\perp^{\,2})}. \qquad (12)$$

Here m_t is the mass of the target particle; P, the beam momentum in the lab.system; a sum is assumed over all possible Reggeons. Inserting (12) into (11) we obtain:

$$A_{3\to 3} = \int_0^x dx_f \int \frac{d^2\vec{k}_{f\perp}}{4(2\pi)^3} \frac{1}{x_f(x-x_f)(1-x+x_f)} \frac{G(s)G(s_f)}{(s-\mu^2)(s_f-\mu_f^2)} \cdot \times$$

$$\times \int_0^x dx' \int \frac{d^2\vec{k}'_{f\perp}}{4(2\pi)^3} \frac{1}{x'_f(x-x'_f)(1-x+x'_f)} \frac{G(s)G(s_f)}{(s'-\mu^2)(s'_f-\mu_f^2)} \times \qquad (13)$$

$$\times \sum_{\beta\beta'} R^{P}_{\beta\beta'}(\vec{k}_\perp^{\,2})(2Pm_t)^{\alpha_P(0)}(1-x)^{\alpha_P(0)-\beta(\vec{k}_\perp^{\,2})-\beta'(\vec{k}_\perp^{\,2})} x_f^{\beta(\vec{k}_\perp^{\,2})} x'_f{}^{\beta'(\vec{k}_\perp^{\,2})}.$$

Neglecting $1-x$ everywhere except the factor $(1-x)^{\alpha_P(0)-\beta(\vec{k}_\perp^{\,2})-\beta'(\vec{k}_\perp^{\,2})}$ we obtain in the leading order in $1-x$:

$$A_{3\to 3} = \sum_{\beta\beta'} \int_0^1 dx_f \int \frac{d^2\vec{k}_{f\perp}}{4(2\pi)^3} \frac{x_f^{\beta(\vec{k}_\perp^{\,2})}}{x_f^2(1-x_f)} \frac{G(s)G(s_f)}{(s-\mu^2)(s_f-\mu_f^2)} \int_0^1 dx'_f \int \frac{d^2\vec{k}'_{f\perp}}{4(2\pi)^3} \frac{x_f^{\beta'(\vec{k}_\perp^{\,2})}}{x'^2_f(1-x'_f)} \times \qquad (14)$$

$$\times \frac{G(s')G(s'_f)}{(s'-\mu^2)(s'_f-\mu_f^2)} R^{P}_{\beta\beta'}(\vec{k}_\perp^{\,2})(2Pm_t)^{\alpha_P(0)}(1-x)^{\alpha_P(0)-\beta(\vec{k}_\perp^{\,2})-\beta'(\vec{k}_\perp^{\,2})}.$$

where

$$s = \frac{m_1^2+(\vec{k}_\perp-\vec{k}_{f\perp})^2}{x_f} + \frac{m_2^2+(\vec{k}_\perp-\vec{k}_{f\perp})^2}{1-x_f},$$

$$s_f = \frac{m_f^2+\vec{k}_{f\perp}^{\,2}}{x_f} + \frac{m_2^2+(\vec{k}_\perp-\vec{k}_{f\perp})}{1-x_f} - \vec{k}_\perp^{\,2}$$

and similar expressions for primed values s', s'_f. Dispersion relation technique allows one to introduce the infinite-momentum frame meson wave function

$$\Psi(x,\vec{k}^{\,2}) = \frac{1}{2\sqrt{x(1-x)}} \frac{G(s)}{s-\mu^2} = \frac{1}{2\sqrt{x(1-x)}}\Psi(s),$$

which is normalized by the condition $\int_0^1 \frac{dx}{x}\int \frac{d^2\vec{k}}{(2\pi)^3}|\Psi|^2 = 1$; the value of $\frac{G(s)}{s-\mu^2} = \Psi(s)$ here is taken to be the same that for the non-relativistic wave function $\Psi_{nr} \sim \frac{G((\vec{k}_1-\vec{k}_2)^2)}{\frac{(\vec{k}_1-\vec{k}_2)^2}{4m}+\epsilon}$, where ϵ is the binding energy of the composite system. Introducing Ψ and Ψ_f into eq.(14), we obtain:

$$A_{3\to 3} \simeq \sum_{\beta\beta'} \int_0^1 dx_f \int \frac{d^2\vec{k}_{f\perp}}{(2\pi)^3} x_f^{\beta(\vec{k}_\perp^2)-1} \Psi(x_f, \vec{k}_{f\perp}^2) \Psi_f(x_f, ((1-x)\vec{k}_\perp - \vec{k}_{f\perp})^2) \times$$

$$\times \int_0^1 dx'_f \int \frac{d^2\vec{k}'_{f\perp}}{(2\pi)^3} x_f'^{\beta'(\vec{k}_\perp^2)-1} \Psi(x'_f, \vec{k}'^2_{f\perp}) \Psi_f(x'_f, (1-x)\vec{k}_\perp - \vec{k}'_{f\perp})^2) \times \qquad (15)$$

$$\times R^P_{\beta\beta'}(0)(2Pm_t)^{\alpha_P(0)}(1-x)^{\alpha_P(0)-\beta(\vec{k}_\perp^2)-\beta'(\vec{k}_\perp^2)}.$$

At $\vec{k}_\perp = 0$ eq. (15) takes a very simple form:

$$A_{3\to 3} \simeq \sum_{\beta\beta'} \int_0^1 dx_f \int \frac{d^2\vec{k}_f}{(2\pi)^3} x_f^{\beta(0)-1} \Psi(x_f, \vec{k}_{f\perp}^2) \Psi_f(x_f, \vec{k}_{f\perp}^2) \times$$

$$\times \int_0^1 dx'_f \int \frac{d^2\vec{k}'_f}{(2\pi)^3} x_f^{\beta(0)-1} \Psi(x'_f, \vec{k}'^2_{f\perp}) \Psi_f(x'_f, \vec{k}'^2_{f\perp}) \times \qquad (16)$$

$$\times R^P_{\beta\beta'}(0)(2Pm_t)^{\alpha_P(0)}(1-x)^{\alpha_P(0)-\beta(0)-\beta'(0)}.$$

Now let us turn to the situation in the multiparticle production process when $x \sim 1/2$. In this case both invariant energies $s_{1f} = (k_1 + k_f)^2$ and $2m_t x_f P$ (or $s_{1'f'} = (k'_1 + k'_f)^2$ and $2m_t x'_f$) in the diagram Fig.6b are large, and $A_{3\to 3}^{(quark)}$ is a usual double-Reggeon amplitude:

$$A_{3\to 3}^{(quark)} = R((\vec{k}_{f\perp} - \vec{k}'_{f\perp})^2) s_{1f}^{\alpha_R((\vec{k}_{f\perp} - \vec{k}'_{f\perp})^2)} (2m_t P x'_f)^{\alpha_P(0)} \times$$

$$\times H((\vec{k}_{f\perp} - \vec{k}'_{f\perp})^2, s_{ff'}) + [x_f \leftrightarrow x'_f, \vec{k}_{f\perp} \leftrightarrow \vec{k}'_{f\perp}], \qquad (17)$$

where

$$s_{1f} = \frac{m_1^2 + (\vec{k}_{f\perp} - \vec{k}_\perp)^2}{1 - x - x_f} x_f + \frac{(m_f^2 + \vec{k}_{f\perp}^2)(1 - x - x_f)}{x_f} - (2\vec{k}_{f\perp} - \vec{k}_\perp)^2 + m_{1\perp}^2 + m_{f\perp}^2$$

$$s_{ff'} = \frac{m_f^2 + \vec{k}_{f\perp}^2}{x'_f} x_f + \frac{m_{f'}^2 + \vec{k}_{f\perp}^2}{x_f} x'_f - (\vec{k}_{f\perp} + \vec{k}'_{f\perp})^2 + m_f^2 + m_{f'}^2$$

and $H((\vec{k}_{f\perp} - \vec{k}'_{f\perp})^2, s_{ff'})$ is a vertex 4-point function with external tails R, f, f', P.

Inserting (17) into (11) and introducing wave functions $\Psi(x, \vec{k}_\perp^2)$ we get:

$$A_{3\to 3} = \int_0^x dx_f \frac{d^2\vec{k}_{f\perp}}{(2\pi)^3} \frac{\Psi(1 - x + x_f, (\vec{k}_{f\perp} - \vec{k}_\perp)^2) \Psi_f(\frac{x_f}{x}, \vec{k}_{f\perp}^2)}{\sqrt{x_f(1 - x + x_f)}} \times$$

$$\times \int_0^x dx'_f \frac{d^2\vec{k}'_{f\perp}}{(2\pi)^3} \frac{\Psi(1 - x + x'_f, (\vec{k}'_{f\perp} - \vec{k}_\perp)^2) \Psi_{f'}(\frac{x'_f}{x}, \vec{k}'^2_{f\perp})}{\sqrt{x'_f(1 - x + x'_f)}} \times$$

$$\times \{R(\vec{k}_{f\perp} - \vec{k}'_{f\perp})^2 (2m_t P x'_f)^{\alpha_P(0)} \cdot H((\vec{k}_{f\perp} - \vec{k}'_{f'\perp})^2, s_{ff'}) \times \qquad (18)$$

$$\times s_{1f}^{\alpha_R((\vec{k}_{f\perp} - \vec{k}'_{f\perp})^2)} + (x_f \leftrightarrow x'_f, \vec{k}_{f\perp} \leftrightarrow \vec{k}'_{f\perp})\}.$$

Generally speaking, $A_{3\to 3}$ in eq. (18) may have a complicated dependence on x and $\vec{k}_\perp^2$ for different initial and secondary mesons. However, there are some simple considerations in the framework of the quark model, which give a possibility of clarifying the structure of $A_{3\to 3}$.

First of all, the integration domain in eq. (18) is determined mainly by the wave functions Ψ and Ψ_f because the amplitude $A_{3\to 3}^{(quark)}$ is a rather smooth function as compared with Ψ. The reason for it is that coloured Reggeon exchange R in Fig.7b is built of gluonic states, which are assumed to be heavier than $q\bar{q}$ states; besides that, the invariant energy in the block H in Fig.7b is comparatively low ($x_f \simeq x'_f$) and its dependence on $s_{ff'}$ and $(\vec{k}_{f\perp} - \vec{k}'_{f\perp})^2$ is to be also smooth.

In the quark model the momentum wave functions of the hadrons-members of one SU(6) multiplet are equal to each other with a good accuracy. Thus, if $A_{3\to 3}^{quark}$ is approximately spin-independent (this is possible in the case of exchange degenerated coloured Reggeons R and of approximate SU(6) symmetry of qq interaction at low energies), from eqs. (18) and (10) we see, that each spin state of the secondary meson is produced with the same cross section, or in other words, the cross section of production of the meson belonging to a given SU(6) multiplet is proportional to the number of its spin states $2J_f + 1$. The resulting set of relations was previously known as the rules of quark statistics (see [41-43] and refs. given therein).

In order to estimate the x-dependence of $A_{3\to 3}$ in the region $x \sim 1/2$ in more detail, let us neglect transverse momentum dependence in the Reggeon R exchange amplitude and assume the block H to be approximately constant. Then $A_{3\to 3}^{quark}$ will be proportional to ($\alpha_{P(0)} \simeq 1$)

$$A_{3\to 3}^{(quark)} \sim x'_f \cdot a\left(\frac{x_f}{1 - x + x_f}\right) + x_f \cdot a\left(\frac{x'_f}{1 - x + x'_f}\right), \qquad (19)$$

where $a(z)$ is some unknown smooth function. At $\vec{k}_\perp = 0$ $A_{3\to 3}$ they may be written as

$$A_{3\to 3} \sim \int_0^x dx_f \int d^2\vec{k}_{f\perp} \frac{\Psi(s)\Psi_f(s_f)}{x_f(x-x_f)(1-x+x_f)} \cdot \int_0^x dx'_f \int d^2\vec{k}'_{f\perp} \frac{\Psi(s')\Psi(s'_f)}{x'_f(x-x'_f)(1-x+x'_f)} \times$$

$$\times x'_f \int_0^1 dz\, a(z)\, \delta\left(z - \frac{x_f}{1-x+x_f}\right) = \qquad (20)$$

$$= \int_0^x \frac{dz}{z} a(z) \int d^2\vec{k}_{f\perp} \frac{(1-z)}{1-x} \frac{\Psi(s)\Psi_f(s_f)}{x-z} \int_0^x dx'_f \int d^2\vec{k}'_{f\perp} \frac{\Psi(s')\Psi(s'_f)}{(x-x'_f)(1-x+x'_f)},$$

where

$$s = \frac{m_1^2 + \vec{k}_{f\perp}^2}{1-x+z\frac{1-x}{1-z}} + \frac{m_2^2 + \vec{k}_{f\perp}^2}{x-z\cdot\frac{1-x}{1-z}}, \qquad \delta_f = x\left(\frac{m_f^2 + \vec{k}_{f\perp}^2}{z\frac{1-x}{1-z}} + \frac{m_2^2 + \vec{k}_{f\perp}^2}{x-z\frac{1-x}{1-z}}\right). \qquad (21)$$

Taking the simplest possible parametrization for Ψ and Ψ_f

$$\Psi(s) = \Psi_f(s) \sim \exp(-R^2 s), \qquad (22)$$

we may estimate $A_{3\to 3}$ in the eq. (20) provided $a(z)$ is given. The value of z expressed the ratio of the longitudinal momentum of the sea quark, picked up by the spectator, to that of the interacting quark ($z = \frac{x_f}{x_1}$). In simple multiperipheral models this value never exceeds 1/2; taking into account that quark q_f is not the fastest one in the ladder (see Fig.6d), we take $a(z) \sim (1-z)^3$. The resulting $A_{3\to 3}$ is then shown in Fig.8; it is interesting to compare it with the x-distribution of the quark-spectator (dashed curve in Fig.8). One can see that these distributions are quite similar in the region $x \sim 1/2$. This property of secondary hadron distributions was previously called "the assumption of soft hadronization" /41,43/; in the context of $1/N_c$ expansion it seems to be a good first approximation.

Let us compare now the expressions for $A_{3\to 3}$ in two cases considered here: $x \to 1$ and $x \sim 1/2$. The main difference between these two cases is that in the first one x-dependence of the cross section is mainly determined by the set of the exchanged Reggeons $R_\beta, R_{\beta'}$ (factor $(1-x)^{\alpha_P - \beta - \beta'}$ in the eq.(13)), while the form of the wave functions Ψ and Ψ_f is not significant. On the contrary, in the second case x-dependence of the cross section is strongly determined by the form of the wave functions almost independent of the exchanged states. Of course, there is an intermediate region of values, where both wave functions and exchanged states play significant role in the formation of x-dependence of the inclusive cross sections. Looking at the

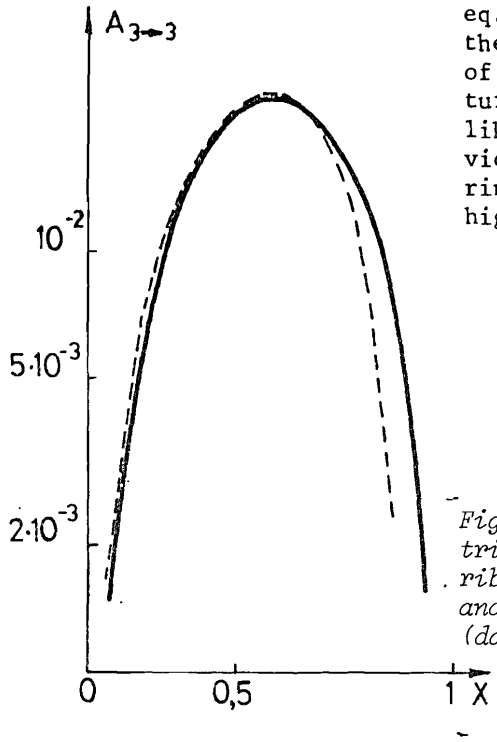

Fig.8. Secondary meson x-distribution, estimated as described in the text (full curve) and that for the quark-spectator (dashed curve).

eq. (11) one may conclude that the two considered behaviours of the inclusive cross section turn one into another smoothly, like, e.g., the resonance behaviour of the low-energy scattering cross section turns into high-energy Regge behaviour.

REFERENCES

1. Levin E.M., Frankfurt L.L. Pis'ma ZhETF, 1965, 2, p.105.
2. Nikolaev N.N. EMC Effect and Breaking of Additivity of Nucleons in the High-Energy Hadron-Nucleus Interactions. Tokyo University Preprint, INS-Rep.-538, 1985.
3. 't Hooft G. Nucl.Phys., 1974, B72, p.461.
4. Veneziano G. Nucl.Phys., 1976, B117, p.519.
5. Witten E. Nucl.Phys., 1979, B160, p.57.
6. Capella A. et al. Phys.Lett., 1979, 81, p.68.
7. Aurenche P., Gonzales-Mestres L. Z.Phys., 1979, C1, p.307.
8. Cohen-Tannoudji G. et al. Phys.Rev., 1980, D21, p.2699.
9. Chin C.B., He Z., Tow D.M. Phys.Rev., 1982, D25, p.2911.
10. Kaidalov A.B., Ter-Martirosyan K.A. Yad.Fiz., 1984, 39, p.1545.
11. Lipkin M.J., Sheck F. Phys.Rev.Lett., 1966, 16, p.71.
12. Kokkedee J.J.J., Van Hove L. Nuovo Cim., 1966, 42, p.711.
13. Satz H. Phys.Lett., 1967, B25, p.220.
14. Anisovich V.V., Gerasyuta S.M. Preprint LNPI-992, 1984 (in Russian).

15. De Rujula A., Georgi H., Glashow S.L. Phys.Rev., 1975, D12, p.147.
16. Glashow S.L. Particle Physics Far from High Energy Frontier. Harward Preprint, HUPT-80/A089, 1980.
17. Isgur N., Karl G. Phys.Lett., 1977, 72B, p.109.
18. Shekhter V.M. Yad.Fiz., 1981, 33, p.817.
19. Elias V., Scardon M.D. Phys.Rev., 1984, D30, p.647.
20. Altarelli G. et al. Nucl.Phys., 1974, B69, p.531.
21. Anisovich V.V. Strong Interaction Processes at High Energies and Quark-Parton Model. In: Proc. of the IV Winter LNPI School, Leningrad, 1974, vol.III (in Russian).
22. Kanki T. Progr.Theor.Phys., 1976, 56, p.1885.
23. Hwa R.C. Phys.Rev., 1980, D22, p.759,1593.
24. Ma E. Phys.Rev., 1978, D17, p.623.
25. Shuryak E.V. Nucl.Phys., 1980, B203, p.93, 116, 140.
26. Miransky V.A., Fomin P.I. Elem.Chast. i Atom. Yad., 1985, 16, p.469.
27. Parisi G., Petronzio R. Phys.Lett., 1980, B94, p.51.
28. Gershtein S.S., Likhoded A.A., Prokoshkin Yu.D. Z.Phys., 1984, C24, p.305.
29. Berg B., Billoire A. Phys.Lett., 1982, B113, p.65.
30. Cornwall J., Soni A. Phys.Lett., 1983, B120, p.431.
31. Harrington D.R., Pagnamenta A. Phys.Rev., 1968, 173, p.1599.
32. Levin E.M. et al. Preprint LNPI-444, Leningrad, 1978 (in Russian).
33. Anisovich V.V. Proc. of the XIV LNPI Winter School, Leningrad, 1979 (in Russian).
34. McCoy B.M., Wu T.T. Phys.Rev.Lett., 1975, 35, p.604.
35. Kuraev E.A., Lipatov L.N., Fadin V.S. ZheTF, 1976, 71, p.84; 1977, 72, p.377.
36. Balitsky Ya.Ya., Lipatov L.N., Fadin V.S. Proc. of the XIV LNPI Winter School, Leningrad, 1979.
37. Braun V.M. Yad.Fiz., 1985, 41, p.405.
38. Anisovich V.V., Dakhno L.G., Volkovitsky P.E. Phys.Lett., 1972, 42B, p.224.
39. Kaidalov A.B., Kondratyuk L.A. Nucl.Phys., 1973, B56, p.90.
40. Anisovich V.V., Dakhno L.G. Nucl.Phys., 1975, B85, p.208.
41. Anisovich V.V. et al. Uspekhi Fiz.Nauk, 1984, 144, p.533.
42. Lipkin H.J. Preprint ANL-HEP-CP-84-75, 1984.
43. Anisovich V.V. et al. Quark Model and High Energy Collisions. World Scientific, Singapore, 1985.

Received by Publishing Department
on July 2, 1986.

Анисович В.В. и др. E2-86-437

$1/N_c$-разложение, кварковая модель и столкновения адронов при высоких энергиях

В рамках гипотезы о глюонном короткодействии и выполнении правил $1/N_c$ разложения рассматриваются процессы мягкого столкновения адронов при высокой энергии. Показано, что в этом случае возникает схема аддитивной кварковой модели, дополненная сравнительно большими эффектами цветового экранирования. Цветовое экранирование ответственно за неестественное нарушение соотношения Левина - Франфурта [1] и, в случае существования в ядрах многокварковых мешков, за эффективное увеличение сечения взаимодействия адронов с нуклонами ядер [2]. Рассматривается механизм образования фрагментации частиц в процессе множественного рождения адронов.

Работа выполнена в Лаборатории теоретической физики ОИЯИ.

Сообщение Объединенного института ядерных исследований. Дубна 1986

Anisovich V.V. et al. E2-86-437

$1/N_c$ Expansion, Quark Model and Hadron Collisions at High Energies

Soft hadron collision processes at high energies are considered, supposing the short-rangeness of gluon interactions and that the rules of $1/N_c$ expansion are fulfilled. It is shown, that these considerations lead to the scheme of the additive quark model with some relatively large additional effects of colour screening. This colour screening is responsible for the unnatural breaking of the Levin-Frankfurt condition [1] and also for the effective increase of cross sections for hadron-nucleus interactions [2] if quark bags in nuclei exist. The formation mechanism of fragmentational particles is considered in multiple hadron production processes.

The investigation has been performed at the Laboratory of Theoretical Physics, JINR.

Communication of the Joint Institute for Nuclear Research. Dubna 1986